# Observation of Two Resonant Structures in $e^+e^- \to \pi^+\pi^-\psi(2S)$ via Initial State Radiation at Belle

X. L. Wang,[10] C. Z. Yuan,[10] C. P. Shen,[10] P. Wang,[10] I. Adachi,[9] H. Aihara,[43]
K. Arinstein,[1] T. Aushev,[18, 13] A. M. Bakich,[38] E. Barberio,[21] I. Bedny,[1] V. Bhardwaj,[33]
U. Bitenc,[14] S. Blyth,[25] A. Bondar,[1] A. Bozek,[27] M. Bračko,[20, 14] J. Brodzicka,[9]
T. E. Browder,[8] P. Chang,[26] A. Chen,[24] K.-F. Chen,[26] B. G. Cheon,[7] C.-C. Chiang,[26]
R. Chistov,[13] I.-S. Cho,[48] S.-K. Choi,[6] Y. Choi,[37] J. Dalseno,[21] M. Danilov,[13] M. Dash,[47]
A. Drutskoy,[3] S. Eidelman,[1] D. Epifanov,[1] N. Gabyshev,[1] A. Go,[24] G. Gokhroo,[39] H. Ha,[16]
K. Hayasaka,[22] H. Hayashii,[23] M. Hazumi,[9] D. Heffernan,[32] Y. Hoshi,[41] W.-S. Hou,[26]
H. J. Hyun,[17] T. Iijima,[22] K. Inami,[22] A. Ishikawa,[34] H. Ishino,[44] R. Itoh,[9] Y. Iwasaki,[9]
D. H. Kah,[17] J. H. Kang,[48] H. Kawai,[2] T. Kawasaki,[29] H. Kichimi,[9] H. O. Kim,[37]
S. K. Kim,[36] Y. J. Kim,[5] K. Kinoshita,[3] S. Korpar,[20, 14] P. Križan,[19, 14] P. Krokovny,[9]
R. Kumar,[33] C. C. Kuo,[24] A. Kuzmin,[1] J. S. Lange,[4] J. S. Lee,[37] M. J. Lee,[36]
S. E. Lee,[36] T. Lesiak,[27] A. Limosani,[21] S.-W. Lin,[26] Y. Liu,[5] D. Liventsev,[13]
F. Mandl,[11] S. McOnie,[38] T. Medvedeva,[13] K. Miyabayashi,[23] H. Miyake,[32] H. Miyata,[29]
R. Mizuk,[13] T. Mori,[22] E. Nakano,[31] M. Nakao,[9] H. Nakazawa,[24] Z. Natkaniec,[27]
S. Nishida,[9] O. Nitoh,[46] S. Noguchi,[23] S. Ogawa,[40] T. Ohshima,[22] S. Okuno,[15]
S. L. Olsen,[8, 10] H. Ozaki,[9] P. Pakhlov,[13] G. Pakhlova,[13] H. Palka,[27] C. W. Park,[37]
H. Park,[17] K. S. Park,[37] R. Pestotnik,[14] L. E. Piilonen,[47] A. Poluektov,[1] H. Sahoo,[8]
Y. Sakai,[9] O. Schneider,[18] A. Sekiya,[23] M. E. Sevior,[21] M. Shapkin,[12] H. Shibuya,[40]
J.-G. Shiu,[26] B. Shwartz,[1] J. B. Singh,[33] A. Sokolov,[12] A. Somov,[3] S. Stanič,[30]
M. Starič,[14] T. Sumiyoshi,[45] F. Takasaki,[9] K. Tamai,[9] M. Tanaka,[9] G. N. Taylor,[21]
Y. Teramoto,[31] I. Tikhomirov,[13] S. Uehara,[9] K. Ueno,[26] T. Uglov,[13] Y. Unno,[7] S. Uno,[9]
P. Urquijo,[21] G. Varner,[8] S. Villa,[18] A. Vinokurova,[1] C. C. Wang,[26] C. H. Wang,[25]
Y. Watanabe,[15] E. Won,[16] B. D. Yabsley,[38] A. Yamaguchi,[42] Y. Yamashita,[28]
M. Yamauchi,[9] C. C. Zhang,[10] Z. P. Zhang,[35] V. Zhilich,[1] V. Zhulanov,[1] and A. Zupanc[14]

(The Belle Collaboration)

[1]*Budker Institute of Nuclear Physics, Novosibirsk*
[2]*Chiba University, Chiba*
[3]*University of Cincinnati, Cincinnati, Ohio 45221*
[4]*Justus-Liebig-Universität Gießen, Gießen*
[5]*The Graduate University for Advanced Studies, Hayama*
[6]*Gyeongsang National University, Chinju*
[7]*Hanyang University, Seoul*
[8]*University of Hawaii, Honolulu, Hawaii 96822*
[9]*High Energy Accelerator Research Organization (KEK), Tsukuba*
[10]*Institute of High Energy Physics,*

*Chinese Academy of Sciences, Beijing*

[11]*Institute of High Energy Physics, Vienna*

[12]*Institute of High Energy Physics, Protvino*

[13]*Institute for Theoretical and Experimental Physics, Moscow*

[14]*J. Stefan Institute, Ljubljana*

[15]*Kanagawa University, Yokohama*

[16]*Korea University, Seoul*

[17]*Kyungpook National University, Taegu*

[18]*Ecole Polytécnique Fédérale Lausanne, EPFL, Lausanne*

[19]*University of Ljubljana, Ljubljana*

[20]*University of Maribor, Maribor*

[21]*University of Melbourne, School of Physics, Victoria 3010*

[22]*Nagoya University, Nagoya*

[23]*Nara Women's University, Nara*

[24]*National Central University, Chung-li*

[25]*National United University, Miao Li*

[26]*Department of Physics, National Taiwan University, Taipei*

[27]*H. Niewodniczanski Institute of Nuclear Physics, Krakow*

[28]*Nippon Dental University, Niigata*

[29]*Niigata University, Niigata*

[30]*University of Nova Gorica, Nova Gorica*

[31]*Osaka City University, Osaka*

[32]*Osaka University, Osaka*

[33]*Panjab University, Chandigarh*

[34]*Saga University, Saga*

[35]*University of Science and Technology of China, Hefei*

[36]*Seoul National University, Seoul*

[37]*Sungkyunkwan University, Suwon*

[38]*University of Sydney, Sydney, New South Wales*

[39]*Tata Institute of Fundamental Research, Mumbai*

[40]*Toho University, Funabashi*

[41]*Tohoku Gakuin University, Tagajo*

[42]*Tohoku University, Sendai*

[43]*Department of Physics, University of Tokyo, Tokyo*

[44]*Tokyo Institute of Technology, Tokyo*

[45]*Tokyo Metropolitan University, Tokyo*

$^{46}$*Tokyo University of Agriculture and Technology, Tokyo*

$^{47}$*Virginia Polytechnic Institute and State University, Blacksburg, Virginia 24061*

$^{48}$*Yonsei University, Seoul*

(Dated: October 26, 2018)

## Abstract

The cross section for $e^+e^- \to \pi^+\pi^-\psi(2S)$ between threshold and $\sqrt{s} = 5.5$ GeV is measured using 673 fb$^{-1}$ of data on and off the $\Upsilon(4S)$ resonance collected with the Belle detector at KEKB. Two resonant structures are observed in the $\pi^+\pi^-\psi(2S)$ invariant mass distribution, one at $4361 \pm 9 \pm 9$ MeV/$c^2$ with a width of $74 \pm 15 \pm 10$ MeV/$c^2$, and another at $4664 \pm 11 \pm 5$ MeV/$c^2$ with a width of $48 \pm 15 \pm 3$ MeV/$c^2$, if the mass spectrum is parameterized with the coherent sum of two Breit-Wigner functions. These values do not match those of any of the known charmonium states.

In a recently reported study of the initial state radiation ($ISR$) process, $e^+e^- \to \gamma_{ISR}\pi^+\pi^- J/\psi$, the BaBar Collaboration observed an accumulation of events near 4.26 GeV/$c^2$ in the invariant-mass spectrum of $\pi^+\pi^- J/\psi$ [1] that they attributed to a possible new resonance, the $Y(4260)$. This structure was also observed by the CLEO [2] and Belle Collaborations using the same technique [3]; in addition, there is a broad structure near 4.05 GeV/$c^2$ in the Belle data. In a subsequent search for the $Y(4260)$ in the $e^+e^- \to \gamma_{ISR}\pi^+\pi^-\psi(2S)$ process, the BaBar Collaboration observed a different structure at $m = 4324 \pm 24$ MeV/$c^2$ with a width of $172 \pm 33$ MeV/$c^2$ [4] that is neither consistent with the $Y(4260) \to \pi^+\pi^-\psi(2S)$ peak nor with $\psi(4415) \to \pi^+\pi^-\psi(2S)$ decay. There are now more observed $J^{PC} = 1^{--}$ states than predicted by potential models [5] in the mass region between 3.8 GeV/$c^2$ and 4.5 GeV/$c^2$; it is possible that one or more of these new states are exotic. However, it should be noted that other interpretations that do not require resonances have been proposed [6].

In this Letter, we report an investigation of the $e^+e^- \to \pi^+\pi^-\psi(2S)$ process using $ISR$ events observed with the Belle detector [7] at the KEKB asymmetric-energy $e^+e^-$ (3.5 on 8 GeV) collider [8]. Here $\psi(2S)$ is reconstructed in the $\pi^+\pi^- J/\psi \to \pi^+\pi^-\ell^+\ell^-$ ($\ell = e, \mu$) final state. The integrated luminosity used in this analysis is 673 fb$^{-1}$. About 90% of the data were collected at the $\Upsilon(4S)$ resonance ($\sqrt{s} = 10.58$ GeV), and the rest were taken at a center-of-mass (CM) energy 60 MeV below the $\Upsilon(4S)$ peak.

We use the PHOKHARA event generator [9] to simulate the process $e^+e^- \to \gamma_{ISR}\pi^+\pi^-\psi(2S)$. In the generator, one or two photons may be emitted before forming the resonance $X$, which then decays to $\pi^+\pi^-\psi(2S)$, with $\psi(2S) \to \pi^+\pi^- J/\psi$ and $J/\psi \to e^+e^-$ or $\mu^+\mu^-$. When generating $X \to \pi^+\pi^-\psi(2S)$, a pure $S$-wave between the $\pi\pi$ system and the $\psi(2S)$, as well as between the $\pi^+$ and $\pi^-$ is assumed. The kinematics of $X$ decays are modelled with the $\pi\pi$ invariant mass distribution observed in our data, while $\psi(2S) \to \pi^+\pi^- J/\psi$ events are generated according to previous measurements [10].

For a candidate event, we require six good charged tracks with zero net charge. A good charged track has transverse momentum greater than 0.1 GeV/$c$ and impact parameters with respect to the interaction point of $dr < 0.5$ cm in the $r$-$\phi$ plane and $|dz| < 5$ (2) cm in the $r$-$z$ plane for pions (leptons). For each charged track, information from different detector subsystems is combined to form a likelihood for each particle species ($i$), $\mathcal{L}_i$ [11]. Tracks with $\mathcal{R}_K = \frac{\mathcal{L}_K}{\mathcal{L}_K + \mathcal{L}_\pi} < 0.4$, are identified as pions with an efficiency of about 95% for the tracks of interest. Similar likelihood ratios are formed for electron and muon identification. For electrons from $J/\psi \to e^+e^-$, both tracks are required to have $\mathcal{R}_e > 0.1$. For muons from $J/\psi \to \mu^+\mu^-$, one of the tracks is required to have $\mathcal{R}_\mu > 0.95$; in addition, if one of the muon candidates has no muon identification (ID) information, the polar angles of the two muon candidates in the $\pi^+\pi^-\mu^+\mu^-$ center-of-mass system are required to satisfy $|\cos\theta_\mu| < 0.75$, based on a comparison between data and MC simulation. The lepton ID efficiency is about 90% for $J/\psi \to e^+e^-$ and 87% for $J/\psi \to \mu^+\mu^-$. The detection of the $ISR$ photon is not required; instead, we require $|M_{\mathrm{rec}}^2| < 2.0$ (GeV/$c^2$)$^2$, where $M_{\mathrm{rec}}^2$ is the square of the mass recoiling against the six charged particle system assuming that four of them are pions and the other two are either electrons or muons. Events with $\gamma$-conversions are removed by requiring $\mathcal{R}_e < 0.75$ for the $\pi^+\pi^-$ tracks accompanying the $\psi(2S)$.

The dilepton invariant mass distribution (the bremsstrahlung photons in the $e^+e^-$ final state are included) for events that survive these selection requirements is shown in Fig. 1(a); it is fitted with a Gaussian and a second-order polynomial. A dilepton pair is

considered as a $J/\psi$ candidate if its invariant mass $(m_{\ell^+\ell^-})$ is within $\pm 45$ MeV/$c^2$ (the mass resolution is 16 MeV/$c^2$) of the $J/\psi$ nominal mass $(m_{J/\psi})$. If there are multiple $\pi^+\pi^-$ combinations that satisfy the $\psi(2S)$ requirements, the one with $|m_{\pi^+\pi^-\ell^+\ell^-} - m_{\ell^+\ell^-}|$, the mass difference between the $\psi(2S)$ and $J/\psi$ [12], closest to 0.589 GeV/$c^2$ is selected; here $m_{\pi^+\pi^-\ell^+\ell^-}$ is the invariant mass of the $\pi^+\pi^-\ell^+\ell^-$ system. Figure 1(b) shows the $m_{\pi^+\pi^- J/\psi}$ $(= m_{\pi^+\pi^-\ell^+\ell^-} - m_{\ell^+\ell^-} + m_{J/\psi})$ distribution. Fitting with a Gaussian and a second-order polynomial yields a mass resolution of 3 MeV/$c^2$. We define a $\psi(2S)$ signal region as $m_{\pi^+\pi^- J/\psi} \in [3.67, 3.70]$ GeV/$c^2$, and a $\psi(2S)$ mass sideband region as $m_{\pi^+\pi^- J/\psi} \in [3.64, 3.67]$ GeV/$c^2$ or $m_{\pi^+\pi^- J/\psi} \in [3.70, 3.73]$ GeV/$c^2$, which is twice as wide as the signal region.
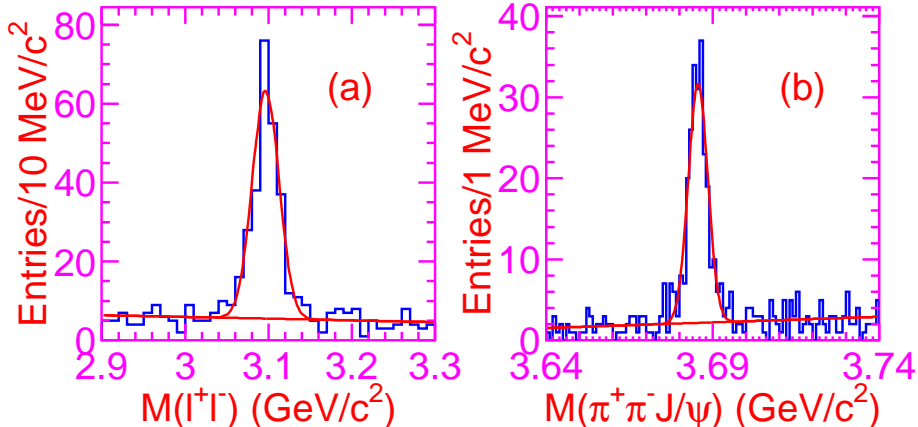


FIG. 1: Invariant mass distributions of $\ell^+\ell^-$ (a) and $\pi^+\pi^- J/\psi$ (b) for selected $\pi^+\pi^-\pi^+\pi^-\ell^+\ell^-$ candidates. The curves show fits described in the text.

Figure 2 shows the $\pi^+\pi^-\psi(2S)$ invariant mass $(m_{\pi^+\pi^-\psi(2S)} = m_{\pi^+\pi^-\pi^+\pi^-\ell^+\ell^-} - m_{\pi^+\pi^-\ell^+\ell^-} + m_{\psi(2S)}$, where $m_{\psi(2S)}$ is the nominal $\psi(2S)$ mass) for selected $\psi(2S)$ events, together with background estimated from the scaled $\psi(2S)$ mass sidebands. Two distinct peaks are evident in Fig. 2, one at 4.36 GeV/$c^2$ and another at 4.66 GeV/$c^2$. As can be seen from the plot, the background determined from the $\psi(2S)$ mass sidebands is very low. Backgrounds not described by the sidebands are negligible; these include $\pi^+\pi^-\psi(2S)$ events, in which the $\psi(2S)$ does not decay to $\pi^+\pi^- J/\psi$ $(J/\psi \to \ell^+\ell^-)$, and events with a $\psi(2S)$ and other particles instead of $\pi^+\pi^-$ in the final state.

Figure 3 shows the $M_{\rm rec}^2$ and polar angle distributions of the $\pi^+\pi^-\psi(2S)$ system in the $e^+e^-$ CM frame for $\pi^+\pi^-\psi(2S)$ events with $m_{\pi^+\pi^-\psi(2S)} \in [4.0, 5.5]$ GeV/$c^2$. The data agree with the MC simulation (shown as histograms) well, indicating that the signal events are produced via $ISR$. Figure 4 shows the $\pi^+\pi^-$ invariant mass distributions for events with $m_{\pi^+\pi^-\psi(2S)} \in [4.0, 4.5]$ GeV/$c^2$, and $m_{\pi^+\pi^-\psi(2S)} \in [4.5, 4.9]$ GeV/$c^2$. In both cases, the mass distributions differ from the phase-space expectation and tend to be concentrated at high mass. In the high mass resonance region, most of the $\pi^+\pi^-$ candidates are consistent with a $f_0(980)$ decay.

An unbinned maximum likelihood fit that includes two coherent $P$-wave Breit-Wigner (BW) functions and a constant, incoherent background is applied to the $\pi^+\pi^-\psi(2S)$ mass spectrum in Fig. 2. The BW width of each resonance is assumed to be constant and an overall three-body phase-space factor is applied. In the fit, the BW shapes are modified by the effective luminosity [13] and $m_{\pi^+\pi^-\psi(2S)}$-dependent efficiency, which increases with
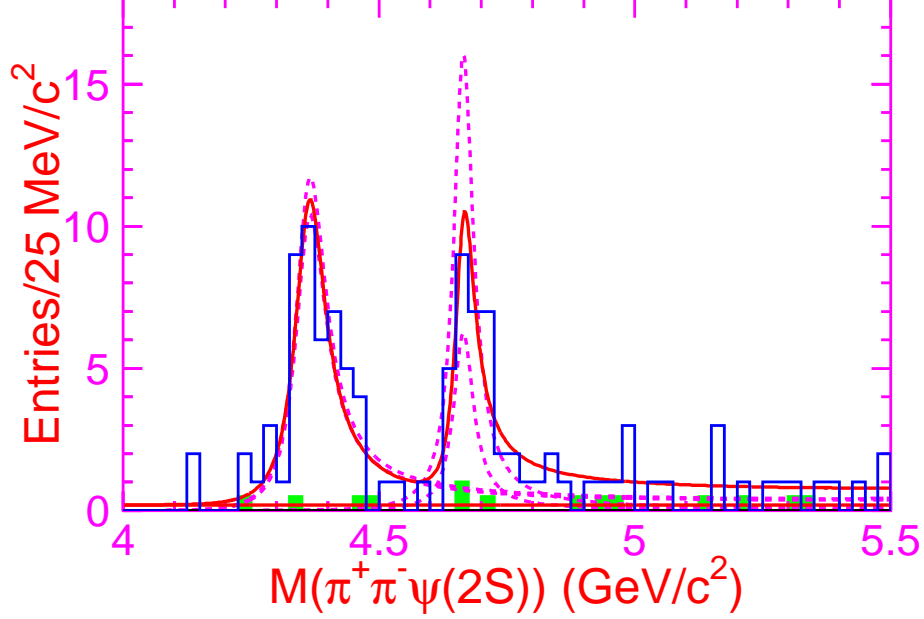
FIG. 2: The $\pi^+\pi^-\psi(2S)$ invariant mass distribution for events that pass the $\psi(2S)$ selection. The open histogram is the data while the shaded histogram is the normalized $\psi(2S)$ sidebands. The curves show the best fit with two coherent resonances together with a background term and the contribution from each component. The interference between the two resonances is not shown. The two dashed curves at each peak show the two solutions (see text).
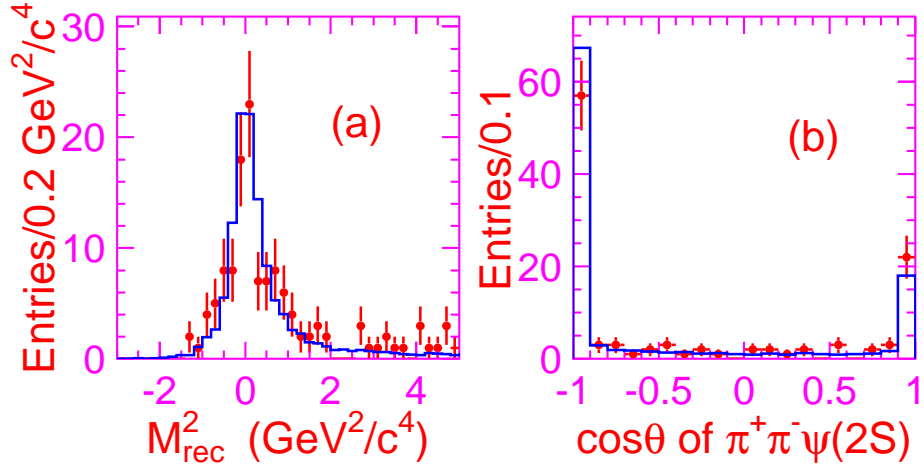


FIG. 3: (a) The $M^2_{\rm rec}$ and (b) polar angle distributions of the $\pi^+\pi^-\psi(2S)$ system in the $e^+e^-$ CM frame for the $\pi^+\pi^-\psi(2S)$ events with $m_{\pi^+\pi^-\psi(2S)} \in [4.0, 5.5]$ GeV/$c^2$. The points with error bars are data, and histograms are from MC simulation.

$m_{\pi^+\pi^-\psi(2S)}$ from 3% at 4.3 GeV/$c^2$ to 5% at 4.7 GeV/$c^2$. The effects of mass resolution, which is determined from MC simulation to be 3 MeV/$c^2$-6 MeV/$c^2$ over the full mass range, are small compared with the widths of the observed structures, and therefore are neglected.

Figure 2 shows the fit results with two solutions with equally good fit quality. In these two solutions, the masses and widths of the resonant structures are the same, but their partial widths to $e^+e^-$ and the relative phase between the two resonant structures are different (see
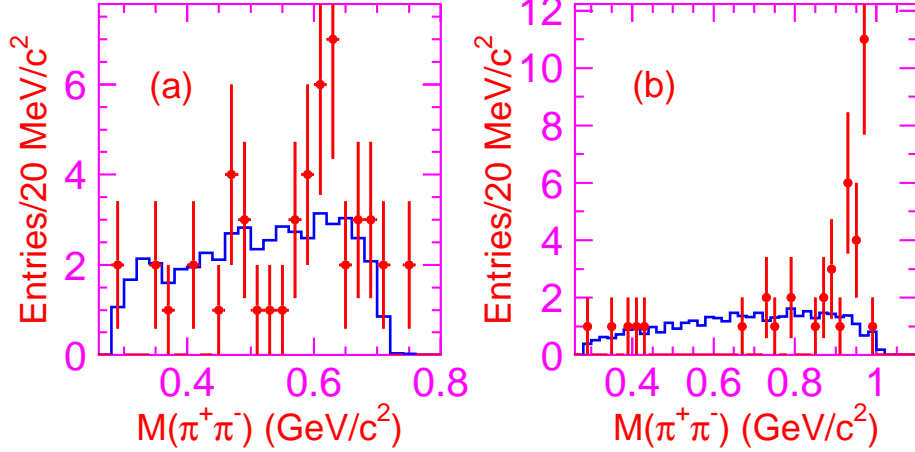
FIG. 4: $\pi^+\pi^-$ invariant mass distributions of events in different $\pi^+\pi^-\psi(2S)$ mass regions. (a): $4.0$ GeV/$c^2 < m_{\pi^+\pi^-\psi(2S)} < 4.5$ GeV/$c^2$, and (b): $4.5$ GeV/$c^2 < m_{\pi^+\pi^-\psi(2S)} < 4.9$ GeV/$c^2$. Points with error bars are data while the histograms are MC simulation with the phase-space distribution generated at $\sqrt{s} = 4.4$ GeV (a) and $4.7$ GeV (b).

TABLE I: Results of the fits to the $\pi^+\pi^-\psi(2S)$ invariant mass spectrum. The first errors are statistical and the second systematic. $M$, $\Gamma_{\text{tot}}$, and $\mathcal{B} \cdot \Gamma_{e^+e^-}$ are the mass (in MeV/$c^2$), total width (in MeV/$c^2$), product of the branching fraction to $\pi^+\pi^-\psi(2S)$ and the $e^+e^-$ partial width (in eV/$c^2$), respectively. $\phi$ is the relative phase between the two resonances (in degrees).

| Parameters | Solution I | Solution II |
|---|---|---|
| $M(Y(4360))$ | $4361 \pm 9 \pm 9$ | |
| $\Gamma_{\text{tot}}(Y(4360))$ | $74 \pm 15 \pm 10$ | |
| $\mathcal{B} \cdot \Gamma_{e^+e^-}(Y(4360))$ | $10.4 \pm 1.7 \pm 1.5$ | $11.8 \pm 1.8 \pm 1.4$ |
| $M(Y(4660))$ | $4664 \pm 11 \pm 5$ | |
| $\Gamma_{\text{tot}}(Y(4660))$ | $48 \pm 15 \pm 3$ | |
| $\mathcal{B} \cdot \Gamma_{e^+e^-}(Y(4660))$ | $3.0 \pm 0.9 \pm 0.3$ | $7.6 \pm 1.8 \pm 0.8$ |
| $\phi$ | $39 \pm 30 \pm 22$ | $-79 \pm 17 \pm 20$ |

Table I) [14]. The interference is constructive for one solution and destructive for the other. To determine the goodness of fit, we bin the data so that the expected number of events in a bin is at least seven and then calculate a $\chi^2/ndf = 4.7/3$ corresponding to a C.L. of 19%. The background level from the fit is $0.19 \pm 0.14$ events per 25 MeV/$c^2$ bin, in good agreement with the $\psi(2S)$ mass sideband estimate of $0.12 \pm 0.05$. The significance of each resonance is estimated by comparing the likelihood of fits with and without that resonance included. We obtain a statistical significance of more than $8\sigma$ for the first peak (hereafter referred to as the $Y(4360)$), and $5.8\sigma$ for the second one (the $Y(4660)$).

The systematic errors in the mass and width measurements are dominated by the choice of parameterization of the resonances, especially the mass dependence of the widths; the range of changes in the fitted values for different parameterizations is reflected in the errors listed in Table I. Other sources of systematic error, such as the mass resolution and the

7

mass scale, are negligible.

The uncertainties in $\mathcal{B} \cdot \Gamma_{e^+e^-}$ due to the choice of parameterization are 7% for the $Y(4360)$ and 10% or 3% for the two $Y(4660)$ solutions. There are other sources of systematic errors for the $\mathcal{B} \cdot \Gamma_{e^+e^-}$ measurement. The particle ID uncertainty, measured using the $e^+e^- \to \psi(2S) \to \pi^+\pi^- J/\psi$ samples [3], is 5.0%; the uncertainty in the tracking efficiency is 1%/track; the uncertainties in the $J/\psi$ mass, $\psi(2S)$ mass, and $M_{\rm rec}^2$ requirements are also measured with a control sample of $e^+e^- \to \psi(2S) \to \pi^+\pi^- J/\psi$ events. For these events, the MC efficiency is found to be higher than in data by $(4.3 \pm 0.5)\%$; a correction factor is applied to the final results and 0.5% is taken as the associated systematic error.

Belle measures luminosity with 1.4% precision while the uncertainty of the radiator in the PHOKHARA program is 0.1% [13]. The main remaining uncertainty in PHOKHARA [9] is associated with the modelling of the $\pi^+\pi^-$ mass spectrum. A MC simulation with $\pi^+\pi^-$ invariant mass distributions that reflect the observations shown in Fig. 4 yields an efficiency that is higher than the phase-space simulation by about 9%, which is used in the fits with half of the correction (4.5%) taken as the systematic error. According to the MC simulation, the trigger efficiency for the events surviving the selection criteria is around 98% with an uncertainty smaller than 1%. The uncertainty in the world average [12] values for $\mathcal{B}(\psi(2S) \to \pi^+\pi^- J/\psi)$ is 1.9% and that of $\mathcal{B}(J/\psi \to \ell^+\ell^-) = \mathcal{B}(J/\psi \to e^+e^-) + \mathcal{B}(J/\psi \to \mu^+\mu^-)$ is 1% where we have added the errors of $e^+e^-$ and $\mu^+\mu^-$ modes linearly. Finally, the statistical error in the efficiency is 1.3%. Treating each source as independent and adding them in quadrature, we obtain total systematic errors on $\mathcal{B} \cdot \Gamma_{e^+e^-}$ in the range 10-14% for the two solutions for the $Y(4360)$ and $Y(4660)$, see Table II.

TABLE II: Systematic errors in the $\mathcal{B} \cdot \Gamma_{e^+e^-}$ measurement.

| Source | Relative error (%) |
|---|---|
| Parameterization | 3−10 |
| Particle ID | 5.0 |
| Tracking efficiency | 6 |
| $J/\psi$ mass, $\psi(2S)$ mass, and $M_{\rm rec}^2$ | 0.5 |
| Integrated luminosity | 1.4 |
| $m_{\pi^+\pi^-}$ distribution | 4.5 |
| Trigger efficiency | 1 |
| Branching fractions | 2.1 |
| MC statistics | 1.3 |
| Sum in quadrature | 10−14 |

The cross section for $e^+e^- \to \pi^+\pi^- \psi(2S)$ for each $\pi^+\pi^- \psi(2S)$ mass bin is calculated according to

$$\sigma_i = \frac{n_i^{\rm obs} - n^{\rm bkg}}{\varepsilon_i \mathcal{L}_i \mathcal{B}(\psi(2S) \to \pi^+\pi^- J/\psi)\mathcal{B}(J/\psi \to \ell^+\ell^-)},$$

where $n_i^{\rm obs}$, $\varepsilon_i$, and $\mathcal{L}_i$ are the number of events observed in data, the efficiency, and the effective luminosity in the $i$-th $\pi^+\pi^- \psi(2S)$ mass bin, respectively; $n^{\rm bkg}$ is the number of background events measured in $\psi(2S)$ sidebands, taken as $0.23 \pm 0.09$ events per 50 MeV/$c^2$

8

for all the bins [15]; $\mathcal{B}(\psi(2S) \to \pi^+\pi^- J/\psi) = 31.8\%$ and $\mathcal{B}(J/\psi \to \ell^+\ell^-) = 11.87\%$ are taken from Ref. [12]. The resulting cross sections are shown in Fig. 5, where the error bars include the statistical uncertainties in the signal and the background subtraction [16]. The large error bars at low mass are due to the low efficiencies. The systematic error for the cross section measurement, which includes all the sources listed in Table II except for that from the BW parameterization, is 9.5% and common to all the data points.
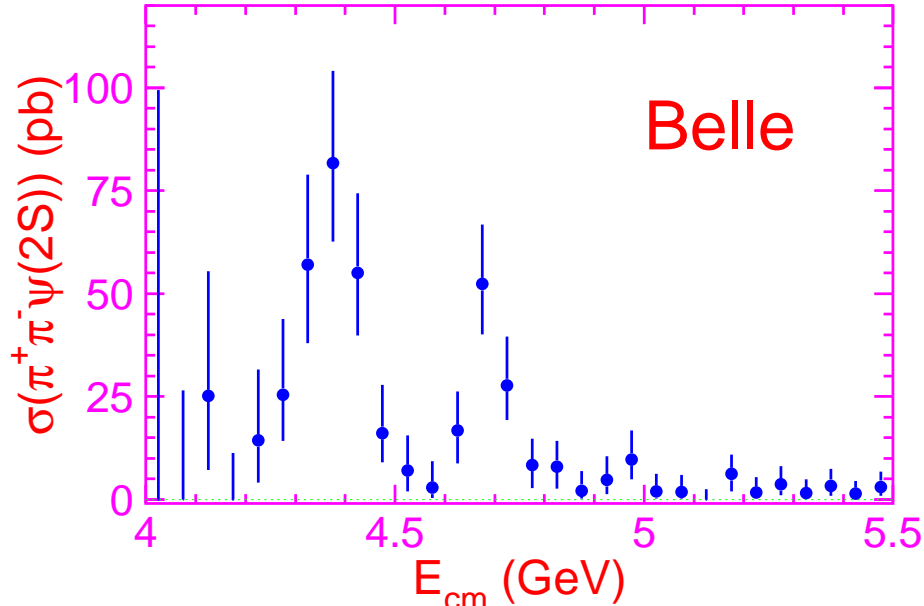


FIG. 5: The measured $e^+e^- \to \pi^+\pi^-\psi(2S)$ cross section for $\sqrt{s} = 4.0$ GeV to 5.5 GeV. The errors are statistical only. Bins without entries have a central value of zero.

In summary, the $e^+e^- \to \pi^+\pi^-\psi(2S)$ cross section is measured from threshold up to 5.5 GeV. The measured cross sections are consistent with results from BaBar [4]. Two distinct resonant structures are observed, one at $m = 4361 \pm 9 \pm 9$ MeV/$c^2$ with a width of $74 \pm 15 \pm 10$ MeV/$c^2$, consistent with the structure observed by BaBar in mass but with a much narrower width, another at $m = 4664 \pm 11 \pm 5$ MeV/$c^2$ with a width of $48 \pm 15 \pm 3$ MeV/$c^2$, that has not been previously observed. The resonant structures reported here are distinct from the ones observed in $e^+e^- \to \pi^+\pi^- J/\psi$ [1, 3]. There are no known vector charmonium states that match these measurements [12, 17]; according to potential model calculations [18, 19], the $4^3S_1$, $5^3S_1$, and $3^3D_1$ charmonium states are expected to be in the mass range close to the two resonances measured. We note that coupled-channel effects and rescattering of pairs of charmed mesons ($D^{(*)}\bar{D}^{(*)}$, $D_s^{(*)}\bar{D}_s^{(*)}$) may affect the above interpretation [6].

[1] BaBar Collaboration, B. Aubert *et al.*, Phys. Rev. Lett. **95**, 142001 (2005).

[2] CLEO Collaboration, Q. He *et al.*, Phys. Rev. D **74**, 091104(R) (2006).

[3] Belle Collaboration, C. Z. Yuan *et al.*, arXiv:0707.2541 [hep-ex], submitted to Phys. Rev. Lett.

[4] BaBar Collaboration, B. Aubert *et al.*, Phys. Rev. Lett. **98**, 212001 (2007).

[5] For a recent review, see for example, E. S. Swanson, Phys. Rept. **429**, 243 (2006).

[6] M. B. Voloshin, arXiv:hep-ph/0602233.

[7] Belle Collaboration, A. Abashian *et al.*, Nucl. Instrum. and Methods Phys. Res. Sect. A **479**, 117 (2002).

[8] S. Kurokawa and E. Kikutani, Nucl. Instrum. and Methods Phys. Res. Sect. A **499**, 1 (2003), and other papers included in this volume.

[9] G. Rodrigo *et al.*, Eur. Phys. J. C **24**, 71 (2002).

[10] BES Collaboration, J. Z. Bai *et al.*, Phys. Rev. D **62**, 032002 (2000).

[11] E. Nakano, Nucl. Instrum. and Methods Phys. Res. Sect. A **494**, 402 (2002).

[12] Particle Data Group, W.-M. Yao *et al.*, J. Phys. G **33**, 1 (2006).

[13] E. A. Kuraev and V. S. Fadin, Sov. J. Nucl. Phys. **41**, 466 (1985) [Yad. Fiz. **41**, 733 (1985)].

[14] Considering the correlation between $\mathcal{B}(\pi^+\pi^-\psi(2S))\cdot\Gamma_{e^+e^-}$ and $\Gamma_{\text{tot}}$, we obtain $\mathcal{B}(\pi^+\pi^-\psi(2S))\cdot\mathcal{B}(e^+e^-) = (14.1\pm3.5\pm1.4)\times10^{-8}$ and $(6.2\pm2.6\pm0.6)\times10^{-8}$ for the $Y(4360)$ and $Y(4660)$, respectively, for solution I; and $\mathcal{B}(\pi^+\pi^-\psi(2S))\cdot\mathcal{B}(e^+e^-) = (15.9\pm3.8\pm1.5)\times10^{-8}$ and $(15.9\pm4.2\pm1.7)\times10^{-8}$ for the $Y(4360)$ and $Y(4660)$, respectively, for solution II.

[15] For the bins with no observed events, the number of background events is taken to be zero when calculating the 68.3% C.L. intervals.

[16] J. Conrad *et al.*, Phys. Rev. D **67**, 012002 (2003).

[17] BES Collaboration, M. Ablikim *et al.*, arXiv:0705.4500 [hep-ex].

[18] E. Eichten *et al.*, Phys. Rev. D **21**, 203 (1980).

[19] S. Godfrey and N. Isgur, Phys. Rev. D **32**, 189 (1985).